NANO LETTERS

pubs.acs.org/NanoLett Letter

One-Step Passivation of Both Sulfur Vacancies and SiO_2 Interface Traps of MoS_2 Device

Byungwook Ahn, Yoonsok Kim, Meeree Kim, Hyang Mi Yu, Jaehun Ahn, Eunji Sim, Hyunjin Ji, Hamza Zad Gul, Keun Soo Kim, Kyuwook Ihm, Hyoyoung Lee, Eun Kyu Kim,* and Seong Chu Lim*

Cite This: *Nano Lett.* 2023, 23, 7927−7933 Read Online

ABSTRACT: Transition metal dichalcogenides (TMDs) benefit electrical devices with spin−orbit coupling and valley- and topology-related properties. However, TMD-based devices suffer from traps arising from defect sites inside the channel and the gate oxide interface. Deactivating them requires independent treatments, because the origins are dissimilar. This study introduces a single treatment to passivate defects in a multilayer MoS_2 FET. By applying back-gate bias, protons from an H−TFSI droplet are injected into the MoS_2, penetrating deeply enough to reach the SiO_2 gate oxide. The characterizations employing low-temperature transport and deep-level transient spectroscopy (DLTS) studies reveal that the trap density of S vacancies in MoS_2 drops to the lowest detection level. The temperature-dependent mobility plot on the SiO_2 substrate resembles that of the h-BN substrate, implying that dangling bonds in SiO_2 are passivated. The carrier mobility on the SiO_2 substrate is enhanced by approximately 2200% after the injection.

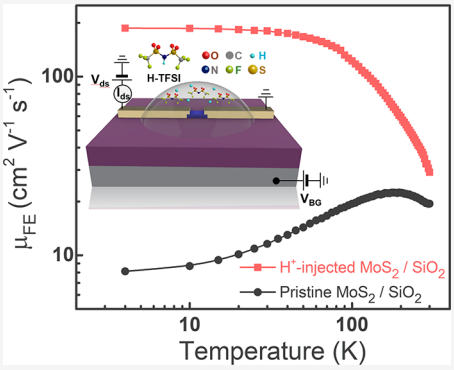

KEYWORDS: *concurrent passivation, MoS_2, proton injection, interface trap, sulfur vacancy, bulk trap*

Recently, 2D layered semiconductors have received worldwide attention, because they are atomically thin and possess no dangling bonds at the surface. Hence, improved device performance is expected from them at the nanoscale.[1] Despite the structural advantages of these materials, the electrical characterization of MoS_2 reveals various problems. For instance, MoS_2 exhibits an n-type behavior attributed to S vacancies. Because of this, the Fermi level is pinned, which enables control of the barrier height of the junction between MoS_2 and the metal electrode.[2] The gap states originating from S vacancies provide nonradiative recombination centers and degrade the photoluminescence (PL) of MoS_2.[3] Furthermore, they contribute to hysteresis in the electrical measurements.[4] The vacancies detrimentally influence both the electrical and optical properties of MoS_2. For these reasons, healing and passivating S defects have drawn considerable attention for achieving an enhanced device performance. For instance, trifluoromethanesulfonimide (H−TFSI) acid, providing S atoms, has been used as a healing agent.[3,5] Treatment with H−TFSI improved the PL intensity of monolayer MoS_2 by 190 times.[5] The electrostatic doping reduces the concentration of trions, consequently amplifying the PL intensity.[6] Treatment of thiol-based self-assembled monolayers (SAMs) on MoS_2 also enhanced carrier mobility.[7−9]

In addition to the S vacancies, devices made of various nanomaterials also suffer from extrinsic factors, including organic impurities, wrinkles, O_2 and H_2O adsorbates, strain, and interface traps.[10,11] One of the most significant extrinsic effects stems from the surface of SiO_2 gate oxide on the Si substrate. Various dangling bonds exist on the SiO_2 gate dielectric. They possess charged impurities that scatter nearby mobile carriers in 2D field-effect transistor (FET) channels, resulting in an inhomogeneous surface potential.[12] The dangling bonds also work as trap states, which cause carrier density and mobility fluctuations by capturing or releasing the channel carriers. Therefore, passivating them on the MoS_2−SiO_2 interface is an important issue.

This study demonstrates a new method that disables scattering by both S vacancies inside bulk MoS_2 and charged impurities on the MoS_2−SiO_2 interface. We introduced protons into a multilayer MoS_2 FET for device applications by applying a gate bias between the back gate and the H−TFSI solution covering the channel. The small hydrogen ions penetrate through both the MoS_2 channel and the MoS_2−SiO_2 interface, and they passivate the S vacancies and ionized dangling bonds in the MoS_2−SiO_2 interface. As a result, the density of S vacancy trap sites was reduced to our lowest detection level, which was confirmed by our deep-level transient spectroscopy (DLTS). Furthermore, the treatment

Received: May 11, 2023
Revised: August 28, 2023
Published: August 30, 2023

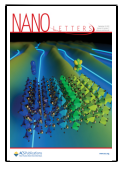

https://doi.org/10.1021/acs.nanolett.3c01753
Nano Lett. 2023, 23, 7927−7933

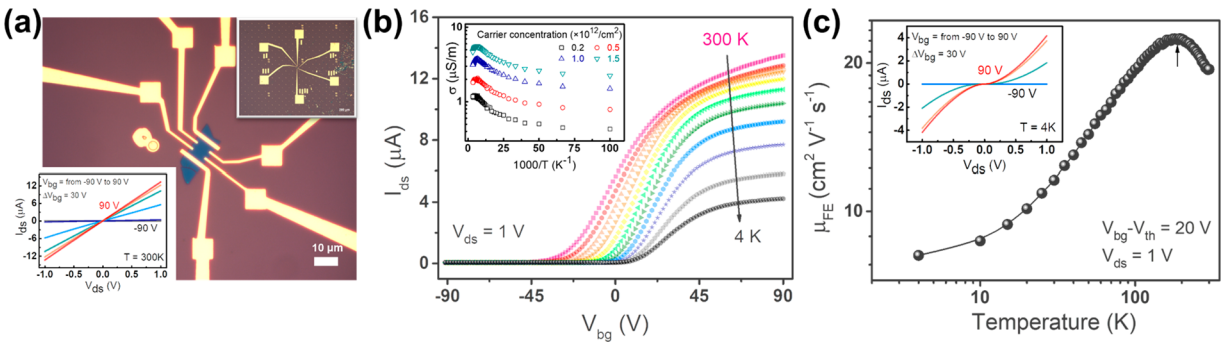

Figure 1. (a) Optical image of a multilayer MoS_2 Hall bar device on a 300 nm-thick SiO_2/Si substrate. The top and bottom insets are an overview of the device and output curves at different V_{bg} values, respectively. (b) Temperature-dependent transfer curves of multilayer MoS_2. The inset is the conductivity (σ) vs 1/temperature (T) plots of multilayer MoS_2 as a function of carrier concentration. (c) Temperature-dependent field effect mobility (μ_{FE}) of the multilayer MoS_2. The inset shows output curves under various V_{bg} concentrations at 4 K.

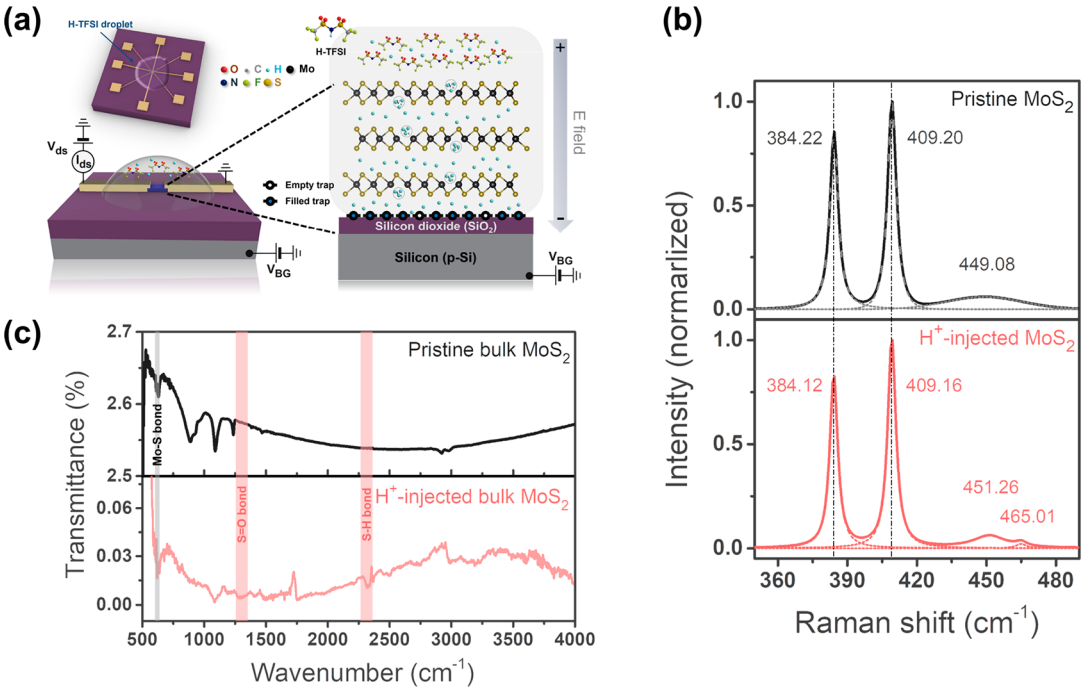

Figure 2. (a) Schematic of H^+ injection into a MoS_2 field-effect transistor (FET). (b) Raman and (c) Fourier transform infrared (FT-IR) spectroscopy analysis before and after H^+ injection into MoS_2.

renders the transport behavior similar to that of the h-BN substrate, i.e., no ionic impurity scattering at low temperatures, even though the device was fabricated on a SiO_2/Si substrate. Our approach is more beneficial compared to the conventional H−TFSI treatment,[3] whose effect relies on S atoms and is limited to only the top surface layer of multilayer MoS_2. Therefore, the remaining MoS_2 layer is open to ionic impurities from the SiO_2/Si substrate.

For the electrical characterization of multilayer MoS_2, we fabricated a 6-bar Hall structure on a 300 nm-thick SiO_2/Si substrate, as shown in Figure 1a [Supporting Information 1]. This device is termed a multilayer MoS_2/SiO_2. The inset of Figure 1a shows that the contact of Cr/Au-MoS_2 is ohmic, although it becomes slightly sublinear at 4 K, as shown in the inset of Figure 1c. Figure 1b presents the transfer curves of the devices measured at different temperatures. The device exhibits a metal−insulator transition (MIT). The conductivity (σ) vs 1/temperature plot, $\sigma \sim 1/T$, in the inset of Figure 1b, details the dependence of the metal−semiconductor transition on both the temperature and carrier concentration. The carrier concentration was calculated using a parallel-capacitance model. At carrier concentrations above 0.5×10^{12} cm^{-2}, multilayer MoS_2 exhibits a metallic behavior, where the conductivity decreases with temperature. The MIT became more pronounced as the carrier concentration increased, as shown in the inset of Figure 1b. This conductivity trend was reversed below 230 K, where the conductivity decreased as the temperature decreased. The turnover temperature coincides with the curves for higher carrier concentrations.

We measured the field-effect mobility μ_{FE} at V_{ds} = 1 V as a function of temperature. The trend of temperature-dependent μ_{FE} is altered with respect to $T \approx 190$ K, as marked by an upward arrow in Figure 1c. At $T > 190$ K, μ_{FE} decreases with increasing temperature, indicating phonon-dominated carrier scattering. In contrast, at $T < 190$ K, μ_{FE} increases with increasing temperature, signifying charged impurity scattering, which is attributed to SiO_2/Si substrate possessing oxygen and Si atoms with unpaired valence electrons. As the temperature

https://doi.org/10.1021/acs.nanolett.3c01753
Nano Lett. 2023, 23, 7927−7933

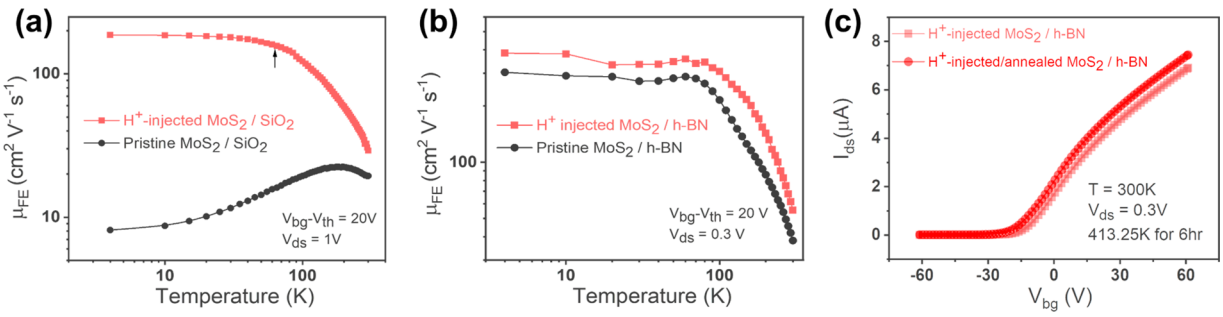

Figure 3. (a) $\log(\mu_{FE})-\log(T)$ of pristine and H^+-injected MoS_2 on a SiO_2 substrate. (b) $\log(\mu_{FE})-\log(T)$ of pristine and H^+-injected MoS_2 on an h-BN substrate. (c) Transfer curve of the H^+-injected MoS_2 device before and after annealing.

decreases, defect scattering gradually dominates over the optical phonon scattering below 190 K. The transition temperature in Figure 1c depends on the concentration of the impurities.[13] For this reason, μ_{FE} is characterized at $|V_{bg} - V_{th}| = 20$ V, at which the carrier concentration $n = 1.445 \times 10^{12}$ cm^{-2}, was obtained using a parallel capacitor model.[14] V_{th} is the threshold voltage.

To passivate the charged impurities in both multilayer MoS_2 and SiO_2 gate dielectrics, we conducted H^+ injection by applying back-gate bias between the Si substrate and H−TFSI, which covers the MoS_2 channel, as shown in Figure 2a. In the H−TFSI solution at 300 K, H−TFSI molecules dissociate into hydrogen ions (H^+) and $TFSI^-$ anions [Supporting Information 2].[15] We did not expect the existence of S ions in the solution. Defects involving S atoms are cured via the catalytic dissociation of TFSI anions near the S vacancy sites.[5] In addition, the decomposition temperature of TFSI is above 573 K.[16] Because all of the experiments were performed at room temperature, the generation of S atoms to restore the vacancy was highly unlikely in the present treatment. The protons in H−TFSI are expected to be attracted toward MoS_2 because of the back-gate bias. The effect of passivation is characterized by comparing the transport behaviors before and after H^+ injection. Our treatment of H−TFSI on a monolayer reproduced the results reported in previous optical studies,[3] which is shown in Supporting Information 3.

We conducted Raman spectroscopy to probe the presence of hydrogen atoms, as shown in Figure 2b. The pristine multilayer MoS_2 presents two characteristic modes at 384.22 and 409.20 cm^{-1}, responsible for in-plane (E^1_{2g}) and out-of-plane (A_{1g}) phonon modes.[17] In addition to these main peaks, a second-order Raman resonant 2LA(M) mode invoked by the collective in-plane atoms is found at 449.08 cm^{-1}. After applying the gate bias, the 2LA mode shifts to higher energy at approximately 451 cm^{-1}, with a new shoulder peak at 465 cm^{-1}, assigned to the A_{2u} mode.[18,19] In pristine MoS_2, the mode is not active, owing to symmetry. However, the adsorption of atoms on the basal plane of MoS_2 can break its symmetry. This contributed to the development of the A_{2u} peak, as shown in Figure 2b. The Raman spectrum is a collection of signals from all of the layers of the multilayer MoS_2, and not only the topmost layer. Therefore, the A_{2u} peak supports the existence of intercalated adatoms in the multilayer MoS_2. Our chemical contains various ions. However, under a gate bias of $V_{bg} = -90$ V, the substances that can be injected into the interlayer gap are limited. Furthermore, the ions passivate both the S vacancies of MoS_2 and the dangling bonds of the SiO_2 gate dielectrics. Therefore, it is proposed that the H^+ ions are responsible for the results shown in Figure 2b.

We cross-checked the injection of H^+ ions into bulk MoS_2 using Fourier transform infrared absorption (FT-IR), as shown in Figure 2c. From a pristine bulk MoS_2, the absorption peak is characterized by Mo−S stretching at 630 cm^{-1}.[20] In addition, absorption peaks arise from organic solvents such as acetone (1090 and 1237 cm^{-1}) and IPA (2915 and 2980 cm^{-1}; C−H stretching vibrational mode) residues,[21] which were used for sample cleaning before FT-IR. After H^+ injection using H−TFSI, the intensity of the organic solvent peaks became negligible [Supporting Information 4]. A key feature after H^+ injection is the presence of thiol (SH) functional groups at 2350 cm^{-1}. The detection of a thiol group is an indication of H^+ ions between the layers inside the multilayer MoS_2 and does not imply substitution for S atoms.[22] The calculations predicted that interstitial H^+ ions could interact with perfect S atoms from the top and bottom layers. Therefore, S−H bonds are present in the interlayer spacing. In addition, the S vacancy site is expected to attract more H^+ ions than perfect S atoms.[23] Thus, the SH peak from MoS_2 injected with H^+ (Figure 2c) may be attributed to protons near the vacancy site with dangling S atoms. The S=O vibrational mode at 1287 cm^{-1} originates from the TFSI molecule.[24] Deep in the multilayer MoS_2 channel is not expected due to the large diameter of the TFSI anions.[24,25]

In contrast to previous studies,[3] our room temperature treatment sustains the probability that TFSI molecules decompose and introduce S ions is low. Moreover, even if S ions are present in the solution, passivation of the sulfur vacancies (V_s) embedded deep in the multilayer MoS_2 channel is not expected due to the large diameter of the TFSI anions.[24] For that reason, our injection method introduced H^+ ions, not S ions. Furthermore, the occupation of H^+ ions at the S vacancy sites can lead to the elimination of gap states.[15] The energy states of S vacancies are usually located 0.45 eV below the conduction band edge. Calculations indicate that the incorporation of H^+ ions shifts the energy states of the S vacancy, V_s, into the conduction band. Thus, no gap states exist in the bandgap.[15]

We analyzed the transport behavior of MoS_2/SiO_2 treated with H^+ ions. Temperature-dependent threshold voltage (V_{th}) curves demonstrate that proton injection caused p-type doping [Supporting Information 5]. In addition, the plots of log (μ_{FE})−log(T) in Figure 3a reveal an enormous difference at low temperatures before and after H^+ injection. In Figure 1c, ionized impurity scattering dominates over its phononic counterpart below 190 K. However, in Figure 3a, at temperatures <70 K (marked by an upward arrow), μ_{FE} saturates, which is attributed to neutral defects at low temperatures. The protonation of multilayer MoS_2 maybe

https://doi.org/10.1021/acs.nanolett.3c01753
Nano Lett. 2023, 23, 7927−7933

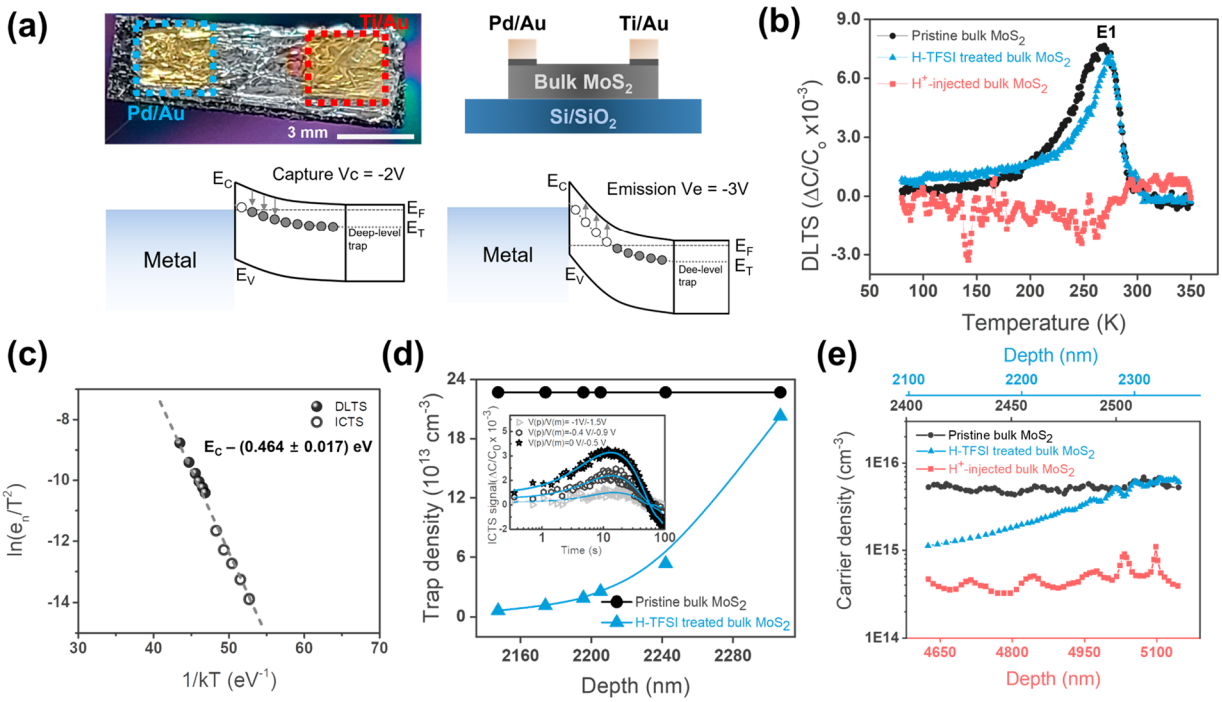

Figure 4. (a) Optical image of actual bulk MoS_2 and a schematic for deep-level transient and isothermal capacitance transient spectroscopy. (b) Deep-level transient spectroscopy (DLTS) signals of pristine/trifluoromethanesulfonimide (H−TFSI)-treated/H^+-injected bulk MoS_2 as a function of temperature. (c) Trap activation energy from DLTS and isothermal capacitance transient spectroscopy (ICTS). Depth profiles of the (d) trap and (e) carrier concentration of bulk MoS_2. The inset in Figure 4d shows ICTS as a function of the gate pulses.

leaves S vacancies in a neutral charge state.[15] At low temperatures, when the phonon population is sufficiently sparse, the collisions of the carriers with the neutral defects outrun those from optical phonons. However, the scattering rate does not depend on the temperature because the number of neutral defect sites does not change with temperature.[26] Whether the ionized defects are neutralized within the SiO_2 gate oxide is unclear.

To clarify the effect of proton injection on SiO_2, we prepared MoS_2 devices on h-BN substrates without charged impurities. The device on h-BN is denoted as multilayer MoS_2/h-BN. A comparison between the pristine and H^+-injected MoS_2/h-BN is shown in Figure 3b. The plots of $\log(\mu_{FE})-\log(T)$ of pristine MoS_2/h-BN reveal no scattering by ionized impurities at low temperatures. Thus, μ_{FE} nearly saturates at approximately 90 K. The comparison of $\log(\mu_{FE})-\log(T)$ between the H^+-injected and pristine MoS_2/h-BN devices indicates that the SiO_2 substrate significantly degrades the carrier mobility, owing to the charged impurities. On the MoS_2/SiO_2 device, the low-temperature μ_{FE} is enhanced by more than an order of magnitude after H^+ injection. Additionally, upon examination of the mobility curve of the MoS_2/h-BN device before and after protonation, we found that the temperature at which mobility saturation occurs did not significantly change (approximately 80−90 K). However, the carrier mobility improved by approximately 30% over the entire temperature range after the H^+ injection. This mobility enhancement from the MoS_2/h-BN device can be explained by passivation of S vacancies by the H^+ ions. Compared to the SiO_2 substrate, the h-BN substrate, which has no dangling bonds, is preferable for device performance. Nevertheless, the growth of large-scale h-BN is limited due to uneven layer thickness from chemical vapor deposition.[27] However, proton injection using gate bias can passivate dangling bonds in the SiO_2 layer, transforming it into an h-BN-like substrate, as demonstrated in Figures 3a and 3b. The concentration of Si and O dangling bonds in the SiO_2 substrate was reduced under H^+-ion-rich growth conditions during atomic layer deposition.[28] Therefore, the passivation of SiO_2 by H^+ injection is consistent with the previous observations.

To confirm the stability of the H^+ injection in multilayer MoS_2, we annealed the device at 413 K for 6 h. Almost the same transfer curve was obtained after annealing, as shown in Figure 3c. The results indicate that the occupation of protons in the S vacancies is chemical rather than physical adsorption. Besides, the durability of the effect of proton injection was evaluated at 300 K. After preserving the proton-injected device within a vacuum chamber for a period of 3 weeks, our observations confirmed that the treatment applied to the MoS_2 device on SiO_2 substrate remained effective, as evidenced by Supporting Information 6.

To explore the effect of H^+ injection on the trap states of MoS_2, we performed deep-level transient spectroscopy (DLTS) and isothermal capacitance transient spectroscopy (ICTS) of bulk MoS_2 samples. Bulk MoS_2 (with a diameter of a few millimeters) was used to probe the penetration depth of the H^+ ions. An asymmetric contact was established on the sample to build a depletion region by employing Pd/Au and Ti/Au electrode metals, as shown in the top panel of Figure 4a. Here, only the Pd/Au electrode on MoS_2 is expected to form a depletion region whose width is controlled using back-gate pulses.

For the DLTS measurements, we applied a pulse gate voltage with a width of 50 ms and a frequency of 10.9862 Hz. The voltage amplitude was modulated from −3 V for emission and −2 V for the capture of electrons by the trap sites, schematically presented in the bottom panel of Figure 4a [Supporting Information 7]. The DLTS signal from the

https://doi.org/10.1021/acs.nanolett.3c01753
Nano Lett. 2023, 23, 7927−7933

pristine bulk MoS_2 reveals a prominent peak, marked as E1 in Figure 4b, during the temperature sweep. The peak in Figure 4b indicates an electron trap state. The existence of electron trap states was double-checked using ICTS. The characteristics of the S vacancies in bulk MoS_2 were obtained by examining the emission rate $e_n = \gamma_n \sigma_n \exp\left[-(E_C - E_T)/k_B T\right]$. E_C is the conduction band edge, κ_B is the Boltzmann constant, E_T is the trap energy, $\gamma_n = 3.25 \times 10^{20}$ $cm^{-2} \cdot s^{-1} \cdot K^{-2} \cdot (m^*/m_0)$, and σ_n is the capture cross-section Here, m^* (0.574 m_0) and m_0 are the effective and free space mass of the electron, respectively.[29] The log plot of the emission rate, written as $\ln(e_n/T^2) = \ln(\gamma_n \sigma_n) - (E_C - E_T)/\ k_B T$, shows the trap energy from the slope in Figure 4c. The trap energy is approximately $E_T = 0.464 \pm 0.017$ eV, which is similar to previous results.[30] The DLTS and ICTS produced consistent results, as shown in Figure 4c. In addition, we estimated the electron capture cross section σ_n using the y-intercept from the plot in Figure 4c. σ_n is approximately 1.13×10^{-16} cm^2, which supports a single point defect. The trap characteristics were further controlled by H−TFSI treatment and H^+ injection, as shown in Figure 4b. When we dipped the pristine bulk MoS_2 into the H−TFSI solution, the DLTS signal was reduced. Surprisingly, after application of a back-gate bias to bulk MoS_2, the DLTS signal was completely depleted, as shown in Figure 4b. Through the temperature sweep from 80 to 350 K, no peaks responsible for the S vacancy are observed in Figure 4b. Spectroscopy indicates that as a result of H^+ ion injection, the trap density is suppressed down to our instrument limit.

In addition to the trap energy, the trap concentration and depth profile of pristine bulk MoS_2 were estimated using the ICTS by changing the emission/capture pulse gate bias, as shown in the inset of Figure 4d. The trap concentration attributed to S vacancies inside pristine bulk MoS_2 is approximately 2.2×10^{14} cm^{-3}, and the concentration is uniform, at least down to 2.3 μm from the surface. Accordingly, the carrier concentration of the pristine bulk MoS_2 shows a consistent profile of approximately 6.0×10^{15} cm^{-3}, as shown in Figure 4e. Here, we used a relative dielectric constant of 7.3 for MoS_2.[31] Next, we scrutinized the trap profiles of bulk MoS_2 dipped in a H−TFSI solution. During dipping of MoS_2 in the solution for 1 h, protons diffused from the surface layer. After the sand was dipped, we observed a significant decrease in trap density, as shown in Figure 4d. Near the surface of bulk MoS_2, the trap concentration reduces to 6.4×10^{12} cm^{-3}, that is, 34 times smaller than the bulk concentration, 2.2×10^{14} cm^{-3}, which is reinstated at 2.3 μm below the surface in Figure 4d. Analogous to the trap concentration, the carrier concentration of bulk MoS_2 is approximately 1.12×10^{15} cm^{-3} and gradually recovers a bulk concentration of 6.0×10^{15} cm^{-3} in Figure 4e. Without biasing, H−TFSI can dope only bulk MoS_2 owing to the diffusion of H^+ ions but is ineffective for passivating the defects. The effects of doping and passivation by H−TFSI differed when a back-gate bias was applied. This effect was confirmed, as shown in Figure 4e, where the carrier density was reduced with depth. When H−TFSI was dropped onto bulk MoS_2, the carrier concentration recovered to its intrinsic level of 2.3 μm below the surface. However, when H^+ ions were injected, the carriers were completely depleted below the surface (Figure 4e). In addition to this hole-doping effect, simply drop-casting the H−TFSI on bulk MoS_2 did not passivate the trap sites, as shown in Figure 4b. After the gate bias was applied to H−TFSI, complete passivation of the trap sites was observed (Figure 4d). According to the theoretical prediction, the passivation of S vacancies with three H^+ ions is not feasible, which is consistent with our observation of the simple doping of bulk MoS_2 into H−TFSI. However, Figure 4b,e shows that the strong gate field facilitated the passivation of S vacancies due to occupation by three H^+ ions.

Recent theoretical calculations predict that the passivation of SiO_2 surfaces possessing −Si and −O dangling bonds is feasible with hydrogen atoms.[12,32] When a pristine SiO_2 surface is exposed to hydrogen atoms, the H atoms bind with the terminated O and Si atoms, resulting in fewer or no trap sites on the SiO_2 surface. In this case, charge transfer between the hydrogen-passivated SiO_2 and MoS_2 can be minimized, and the charge trapping/detrapping between SiO_2 and MoS_2 is relaxed. We conducted an interface trap analysis on MoS_2/SiO_2 devices using 1/f noise, the method of which is described elsewhere.[33] The results in Figure S8 indicate that the interface trap density D_{it} on SiO_2 was significantly reduced after H^+ injection.

Herein, TFSI treatment of monolayer MoS_2 did not increase the carrier mobility due to scattering from the ionic impurities in TFSI [Supporting Information 9]. Therefore, the mobility enhancement in multilayer MoS_2 does not result from the surface layer but from the entire layer. TFSI anions cannot diffuse through the multilayer MoS_2. Thus, the mobility enhancement is affected by ions that are much smaller than the TFSI anions. Therefore, these ions can even reach the SiO_2 substrates. It is plausible that other ions occupied the S vacancies. However, it is highly unlikely that the occupation of the vacancies by these ions passivated the trap sites, as predicted by theoretical calculations.[15] The DLTS results in Figures 4b−e show the absence of the gap state by the S vacancy after the injection of ions that are highly diffusive through the layers. In addition, TSFI is effective for passivating the Si surfaces.[34] The Raman and FT-IR spectroscopy and DLTS data strongly support the deep penetration of protons, which passivate the S vacancies and Si/O dangling bonds of the SiO_2 gate dielectric.

The devices fabricated with two-dimensional (2D) layered structures have shown promising properties that are not accessible with conventional Si devices. However, the lack of controllability in the growth and device fabrication processes leads to detrimental hysteresis during operation, which is attributed to defects in the channel and trap sites at the SiO_2 interface. Suppressing their influence on the channel was sought. In our MoS_2 FET, H^+ ions from H−TFSI penetrate the multilayer MoS_2 and inactivate the S vacancies in MoS_2 as well as the dangling bonds at the SiO_2 interface, both of which have been known to degrade the device performance and are technical and scientific targets to be overcome. SiO_2 substrates have been used as platforms for devices that employ diverse nanomaterials. However, eliminating the ionized functional groups of SiO_2 requires chemical treatment, which subsequently changes the surface states of SiO_2, deteriorating the device fabrication. For this reason, h-BN is the material of choice for gate oxides. Despite the introduction of h-BN, the MoS_2 channel still contains sulfur vacancies. In our approach, the injection of H^+ suppresses the activity of trap sites from the channel and gate dielectric. Moreover, our protonation is more advantageous than hydrogen plasma, which can simultaneously blast S atoms away from the MoS_2. We expect that our approach can be applied to various devices with 2D layered

https://doi.org/10.1021/acs.nanolett.3c01753
Nano Lett. 2023, 23, 7927−7933

materials to investigate the intrinsic electrical properties without any distortion by traps.

■ ASSOCIATED CONTENT

Supporting Information

The Supporting Information is available free of charge at https://pubs.acs.org/doi/10.1021/acs.nanolett.3c01753.

Device fabrication of multilayer MoS_2, preparation of H−TFSI solution and proton injection method, photoluminescence spectra and mapping images, Raman spectra, XPS spectra, FT-IR spectra, threshold voltage, durability test of H^+ injection, DLTS and ICTS analyses, interface trap density, and transport behavior of H−TFSI-treated monolayer MoS_2 (PDF)

■ AUTHOR INFORMATION

Corresponding Authors

Eun Kyu Kim − *Department of Physics, Hanyang University, Seoul 04763, Republic of Korea;* orcid.org/0000-0003-3373-963X; Email: ek-kim@hanyang.ac.kr

Seong Chu Lim − *Department of Energy Science, Sungkyunkwan University, Suwon 16419, Republic of Korea; Department of Smart Fabrication Technology, Sungkyunkwan University, Suwon 16419, Republic of Korea;* orcid.org/0000-0002-0751-1458; Email: seonglim@skku.edu

Authors

Byungwook Ahn − *Department of Energy Science, Sungkyunkwan University, Suwon 16419, Republic of Korea*

Yoonsok Kim − *Department of Physics, Hanyang University, Seoul 04763, Republic of Korea; Institute of Plasma Technology, Korea Institute of Fusion Energy, Gunsan 54004, Republic of Korea*

Meeree Kim − *Department of Chemistry, Sungkyunkwan University, Suwon 16419, Republic of Korea;* orcid.org/0000-0001-9183-0517

Hyang Mi Yu − *Department of Energy Science, Sungkyunkwan University, Suwon 16419, Republic of Korea*

Jaehun Ahn − *Department of Energy Science, Sungkyunkwan University, Suwon 16419, Republic of Korea*

Eunji Sim − *Department of Energy Science, Sungkyunkwan University, Suwon 16419, Republic of Korea*

Hyunjin Ji − *Department of Electrical Engineering, University of Ulsan, Ulsan 44610, Republic of Korea*

Hamza Zad Gul − *Department of Electrical Engineering, Namal University, Mianwali 42250, Pakistan*

Keun Soo Kim − *Department of Physics and Graphene Research Institute, Sejong University, Seoul 05006, Republic of Korea;* orcid.org/0000-0002-4901-6156

Kyuwook Ihm − *Nano & Interface Research Team, Pohang Accelerator Laboratory, Pohang 37673, Republic of Korea;* orcid.org/0000-0003-0075-5772

Hyoyoung Lee − *Department of Chemistry, Sungkyunkwan University, Suwon 16419, Republic of Korea;* orcid.org/0000-0002-8031-0791

Complete contact information is available at: https://pubs.acs.org/10.1021/acs.nanolett.3c01753

Author Contributions

B.W.A fabricated, chemically treated, and conducted both electrical and optical characterizations of MoS_2 devices. Y.K. conducted DLTS and analyzed data. M.K. and H.L. prepared H−TFSI solution. H.M.Y. took FT-IR spectra of MoS_2 before and after H−TFSI treatment. J.A. transferred MoS_2 and graphene flakes on SiO_2 substrate. E.S. and K.W.I. performed chemical analysis of monolayer MoS_2 using XPS. H.J. characterized the noise properties of the devices. H.Z.G. carried out electrical measurements. K.S.K. grew monolayer graphene for the electrodes. E.K.K. and S.C.L. orchestrated experiments, analyzed the data, and prepared the paper.

Notes

The authors declare no competing financial interest.

■ ACKNOWLEDGMENTS

This work was supported by the Commercialization Promotion Agency for R&D outcomes funded by the Ministry of Science and ICT (grant No: RS-2023-00243196) and Basic Science Research Program through the National Research Foundation of Korea (NRF) funded by the Ministry of Education (grant No: NRF-2022R1I1A1A01073120 and NRF-2022M3I8A2085434).

■ REFERENCES

(1) Shen, Y.; Dong, Z.; Sun, Y.; Guo, H.; Wu, F.; Li, X.; Tang, J.; Liu, J.; Wu, X.; Tian, H.; et al. The trend of 2D transistors toward integrated circuits: Scaling down and new mechanisms. *Adv. Mater.* **2022**, *34*, 2201916.

(2) Kim, C.; Moon, I.; Lee, D.; Choi, M. S.; Ahmed, F.; Nam, S.; Cho, Y.; Shin, H.-J.; Park, S.; Yoo, W. J. Fermi level pinning at electrical metal contacts of monolayer molybdenum dichalcogenides. *ACS Nano* **2017**, *11*, 1588−1596.

(3) Amani, M.; Lien, D.-H.; Kiriya, D.; Xiao, J.; Azcatl, A.; Noh, J.; Madhvapathy, S. R.; Addou, R.; KC, S.; Dubey, M.; Cho, K.; Wallace, R. M.; Lee, S.-C.; He, J.-H.; Ager, J. W.; Zhang, X.; Yablonovitch, E.; Javey, A. Near-unity photoluminescence quantum yield in MoS_2. *Science* **2015**, *350*, 1065−1068.

(4) Shu, J.; Wu, G.; Guo, Y.; Liu, B.; Wei, X.; Chen, Q. The intrinsic origin of hysteresis in MoS_2 field effect transistors. *Nanoscale* **2016**, *8*, 3049−3056.

(5) Roy, S.; Choi, W.; Jeon, S.; Kim, D.-H.; Kim, H.; Yun, S. J.; Lee, Y.; Lee, J.; Kim, Y.-M.; Kim, J. Atomic observation of filling vacancies in monolayer transition metal sulfides by chemically sourced sulfur atoms. *Nano Lett.* **2018**, *18*, 4523−4530.

(6) Lien, D.-H.; Uddin, S. Z.; Yeh, M.; Amani, M.; Kim, H.; Ager, J. W., III; Yablonovitch, E.; Javey, A. Electrical suppression of all nonradiative recombination pathways in monolayer semiconductors. *Science* **2019**, *364* (6439), 468−471.

(7) Yu, Z.; Pan, Y.; Shen, Y.; Wang, Z.; Ong, Z.-Y.; Xu, T.; Xin, R.; Pan, L.; Wang, B.; Sun, L.; et al. Towards intrinsic charge transport in monolayer molybdenum disulfide by defect and interface engineering. *Nat. Commun.* **2014**, *5*, 5290.

(8) Makarova, M.; Okawa, Y.; Aono, M. Selective adsorption of thiol molecules at sulfur vacancies on MoS_2 (0001), followed by vacancy repair via S-C dissociation. *J. Phys. Chem. C* **2012**, *116* (42), 22411−22416.

(9) Wiegenstein, C. G.; Schulz, K. H. Methanethiol adsorption on defective MoS_2 (0001) surfaces. *J. Phys. Chem. B* **1999**, *103* (33), 6913−6918.

(10) Liang, J.; Xu, K.; Toncini, B.; Bersch, B.; Jariwala, B.; Lin, Y. C.; Robinson, J.; Fullerton-Shirey, S. K. Impact of Post-Lithography Polymer Residue on the Electrical Characteristics of MoS_2 and WSe_2 Field Effect Transistors. *Advanced Materials Interfaces* **2019**, *6*, 1801321.

(11) Late, D. J.; Liu, B.; Matte, H. R.; Dravid, V. P.; Rao, C. Hysteresis in single-layer MoS_2 field effect transistors. *ACS Nano* **2012**, *6*, 5635−5641.

(12) Sung, H.-J.; Choe, D.-H.; Chang, K.-J. The effects of surface polarity and dangling bonds on the electronic properties of monolayer and bilayer MoS_2 on α-quartz. *New J. Phys.* **2014**, *16*, 113055.
(13) Kim, S.; Konar, A.; Hwang, W.-S.; Lee, J. H.; Lee, J.; Yang, J.; Jung, C.; Kim, H.; Yoo, J.-B.; Choi, J.-Y.; et al. High-mobility and low-power thin-film transistors based on multilayer MoS_2 crystals. *Nat. Commun.* **2012**, *3*, 1011.
(14) Lee, J. H.; Gul, H. Z.; Kim, H.; Moon, B. H.; Adhikari, S.; Kim, J. H.; Choi, H.; Lee, Y. H.; Lim, S. C. Photocurrent switching of monolayer MoS_2 using a metal-insulator transition. *Nano Lett.* **2017**, *17*, 673−678.
(15) Lu, H.; Kummel, A.; Robertson, J. Passivating the sulfur vacancy in monolayer MoS_2. *APL Materials* **2018**, *6*, 066104.
(16) https://www.sigmaaldrich.com/KR/en/sds/sial/15220.
(17) Lee, C.; Yan, H.; Brus, L. E.; Heinz, T. F.; Hone, J.; Ryu, S. Anomalous lattice vibrations of single-and few-layer MoS_2. *ACS Nano* **2010**, *4*, 2695−2700.
(18) Li, Z.; Bretscher, H.; Zhang, Y.; Delport, G.; Xiao, J.; Lee, A.; Stranks, S. D.; Rao, A. Mechanistic insight into the chemical treatments of monolayer transition metal disulfides for photoluminescence enhancement. *Nat. Commun.* **2021**, *12*, 6044.
(19) Qian, Q.; Zhang, Z.; Chen, K. J. In situ resonant raman spectroscopy to monitor the surface functionalization of MoS_2 and WSe_2 for High-K integration: A first-principles study. *Langmuir: the ACS journal of surfaces and colloids* **2018**, *34*, 2882−2889.
(20) Lalithambika, K.; Shanmugapriya, K.; Sriram, S. Photocatalytic activity of MoS_2 nanoparticles: an experimental and DFT analysis. *Appl. Phys. A: Mater. Sci. Process.* **2019**, *125*, 1−8.
(21) Christensen, P. A.; Mashhadani, Z.; Md Ali, A. H. B.; Carroll, M. A.; Martin, P. A. The production of methane, acetone,"Cold" CO and oxygenated species from isopropyl alcohol in a Non-thermal plasma: An in-situ FTIR study. *J. Phys. Chem. A* **2018**, *122*, 4273−4284.
(22) Jiang, Y.; Wang, J.; Wu, J.; Zhang, Y. Preparation of high-performance natural rubber/carbon black/molybdenum disulfide composite by using the premixture of epoxidized natural rubber and cysteine-modified molybdenum disulfide. *Polym. Bull.* **2021**, *78*, 1213−1230.
(23) An, Y.; Kuc, A.; Petkov, P.; Lozada-Hidalgo, M.; Heine, T. On the Chemistry and Diffusion of Hydrogen in the Interstitial Space of Layered Crystals h-BN, MoS_2, and Graphite. *Small* **2019**, *15* (43), 1901722.
(24) Kim, H.; Lien, D.-H.; Amani, M.; Ager, J. W.; Javey, A. Highly stable near-unity photoluminescence yield in monolayer MoS_2 by fluoropolymer encapsulation and superacid treatment. *ACS Nano* **2017**, *11*, 5179−5185.
(25) Zhang, J.; Yang, A.; Wu, X.; van de Groep, J.; Tang, P.; Li, S.; Liu, B.; Shi, F.; Wan, J.; Li, Q.; et al. Reversible and selective ion intercalation through the top surface of few-layer MoS_2. *Nat. Commun.* **2018**, *9*, 5289.
(26) Cui, X.; Lee, G.-H.; Kim, Y. D.; Arefe, G.; Huang, P. Y.; Lee, C.-H.; Chenet, D. A.; Zhang, X.; Wang, L.; Ye, F.; et al. Multi-terminal transport measurements of MoS_2 using a van der Waals heterostructure device platform. *Nature Nanotechnol.* **2015**, *10*, 534−540.
(27) Jang, S. K.; Youn, J.; Song, Y. J.; Lee, S. Synthesis and characterization of hexagonal boron nitride as a gate dielectric. *Sci. Rep.* **2016**, *6*, 30449.
(28) Renz, A.; Vavasour, O. J.; Gammon, P.; Li, F.; Dai, T.; Antoniou, M.; Baker, G.; Bashar, E.; Grant, N.; Murphy, J.; et al. The improvement of atomic layer deposited SiO_2/4H-SiC interfaces via a high temperature forming gas anneal. *Materials Science in Semiconductor Processing* **2021**, *122*, 105527.
(29) Moun, M.; Kumar, M.; Garg, M.; Pathak, R.; Singh, R. Understanding of MoS_2/GaN heterojunction diode and its photodetection properties. *Sci. Rep.* **2018**, *8*, 11799.
(30) Qiu, H.; Xu, T.; Wang, Z.; Ren, W.; Nan, H.; Ni, Z.; Chen, Q.; Yuan, S.; Miao, F.; Song, F.; et al. Hopping transport through defect-induced localized states in molybdenum disulphide. *Nat. Commun.* **2013**, *4*, 2642.
(31) Laturia, A.; Van de Put, M. L.; Vandenberghe, W. G. Dielectric properties of hexagonal boron nitride and transition metal dichalcogenides: from monolayer to bulk. *npj 2D Mater. Appl.* **2018**, *2*, 6.
(32) Ma, X.; Liu, Y.-Y.; Zeng, L.; Chen, J.; Wang, R.; Wang, L.-W.; Wu, Y.; Jiang, X. Defects Induced Charge Trapping/Detrapping and Hysteresis Phenomenon in MoS_2 Field-Effect Transistors: Mechanism Revealed by Anharmonic Marcus Charge Transfer Theory. *ACS Appl. Mater. Interfaces* **2022**, *14*, 2185−2193.
(33) Ji, H.; Yi, H.; Wonkil, S.; Kim, H.; Lim, S. C. Reduced interfacial fluctuation leading enhanced mobility in a monolayer MoS_2 DG FET under low vertical electric field. *Nanotechnology* **2019**, *30*, 345206.
(34) Pointon, A.; Grant, N. E.; Wheeler-Jones, E.; Altermatt, P.; Murphy, J. D. Superacid-derived surface passivation for measurement of ultra-long lifetimes in silicon photovoltaic materials. *Sol. Energy Mater. Sol. Cells* **2018**, *183*, 164−172.

https://doi.org/10.1021/acs.nanolett.3c01753
Nano Lett. 2023, 23, 7927−7933